

# DFT studies of structural preference of coordinated ethylene in $W(CO)_3(PX_3)_2(CH_2=CH_2)$ ( $X = H, CH_3, F, Cl, Br, \text{ and } I$ )

Alireza Ariafard \*

*Department of Chemistry, Islamic Azad University, Center Tehran Branch, Felestin Square, Tehran, Iran*

Received 8 December 2003; accepted 2 April 2004

## Abstract

A set of phosphine complexes of the type  $W(CO)_3(PX_3)_2(CH_2=CH_2)$  ( $X = H, CH_3, F, Cl, Br, \text{ and } I$ ) were investigated by density functional theory method (BP86) to examine the effect of the substituent X on the orientation of C–C vector of the ethylene ligand with respect to one of the metal–ligand bonds as well as the donation and the backdonation in the bonding ligands of phosphine and ethylene. When  $X = CH_3, H, F, \text{ and } Cl$ , the ethylene C–C vector prefers to be coplanar with metal–phosphine bonds, while for the ethylene complexes containing  $PBr_3$  and  $PI_3$  ligands, the structural preference is coplanarity of the ethylene and the metal–carbonyl bonds. The molecular orbital calculations and natural bond orbital analysis were used to examine the structural consequences derived from these complexes. It can be concluded that the structural preferences in the complexes have a clear relation to electronic effects of phosphine ligands. Our calculations for halide phosphine complexes, particularly for  $PBr_3$  and  $PI_3$ , allow us to conclude that in addition to electronic effects, steric factors can also affect the orientation of the ethylene ligand in complexes.

© 2004 Elsevier B.V. All rights reserved.

*Keywords:* Ethylene complexes;  $\pi$ -Backdonation;  $\sigma$ -Donation; DFT study; Phosphine; Tungsten

## 1. Introduction

Alkene complexes have attracted much attention in the past decade because they are considered as important catalysis for a variety of reactions including olefin polymerization [1], hydrogenation [2], and hydroformylation [3]. An accurate knowledge of the nature of the alkene–metal bond is essential for understanding the mechanisms of transition metals catalysts involving an alkene–metal interaction [4].

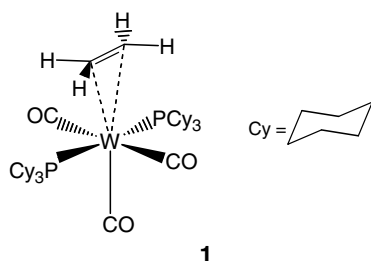
The Dewar–Chatt–Duncanson (DCD) gave a simple description of the transition metal–alkene bonding based on  $\pi$ -donation and metal backdonation [5]. The alkene ligand has only one  $\pi^*$  orbital with suitable symmetry for interaction with metal d orbitals. Ligands having only one low-lying empty orbital available for

$\pi$ -interaction with metal center are called single-face  $\pi$ -accepting ligand, such as  $\eta^1$ -alkenyl,  $\eta^2$ -olefin, and  $\eta^2$ -silane, etc. [6]. A variety of computational studies using different levels of theory have been reported for these types of complexes [6–11].

In 1997, Butts et al. [12] reported the synthesis and structure of  $W(CO)_3(PCy_3)_2(\eta^2-C_2H_4)$  which agrees with structure **1**. An interesting structural feature in this complex is the coplanar orientation of the ethylene and phosphine ligands. Due to the presence of carbonyl ligand, which is a double-face strong  $\pi$ -acceptor ligand, the preference for coplanarity can be explained by maximum utilization of metal d orbitals for backbonding interaction with both the ethylene and carbonyl ligands [6]. Other similar complexes such as  $W(P(OEt)_3)(P(OMe)_3)(CO)_3(\eta^2-CHR=CHR)$  [13] and  $W(PPh_2CH_2CH_2PPh_2)(CO)_3(\eta^2-CHR=CHR)$  [14], where R is  $COOCH_3$ , also indicate the same behavior. However, the extent of the metal–ethylene backbonding interaction can be affected by the substituents on the ethylene ligand as well as the metal center [6,12].

\* Tel.: +98-21-4803708; fax: +98-281-2563931.

E-mail address: [ariafard@yahoo.com](mailto:ariafard@yahoo.com).



The different kinds of phosphines,  $\text{PR}_3$ , can be suitable ligands for such the complexes. These ligands are important because their electronic and steric properties can be altered in wide range by varying R. The phosphines, in addition to  $\sigma$ -donor property (via a hybrid orbital containing a lone pair on phosphorus) are also considered as double-face  $\pi$ -acceptors (via empty  $\sigma^*$  orbitals of the P–R bonds) in which the nature of the R group determines the relative donor/acceptor ability [15]. Recently, the theoretical studies have also been done on complexes containing phosphine ligands [16–18].

The aforementioned points have prompted us to study the rotational barrier of ethylene in phosphine complexes  $\text{W}(\text{CO})_3(\text{PX}_3)_2(\text{CH}_2=\text{CH}_2)$  ( $\text{X} = \text{H}, \text{CH}_3, \text{F}, \text{Cl}, \text{Br}, \text{and I}$ ) to examine the effect of different electronic and steric properties resulted from phosphine ligands on the W–ethylene and W–phosphine interactions using DFT calculations. Following our effort in understanding the W–ethylene and W–phosphine interactions, in this paper, the molecular orbital (MO) calculations and NBO analysis were used to provide a suitable explanation.

## 2. Computational method

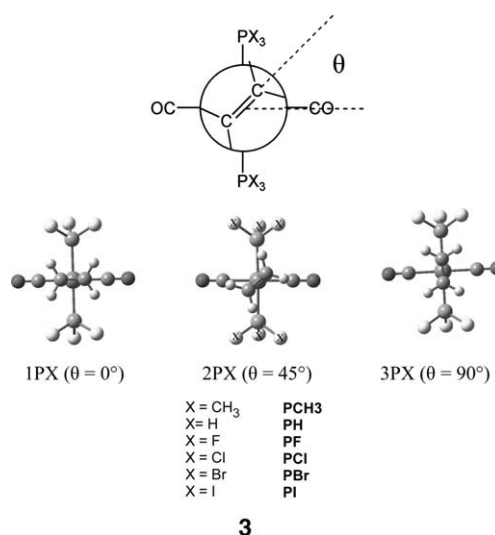
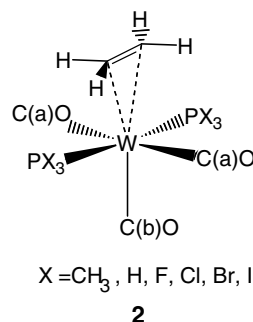
Geometry optimizations of all the phosphine complexes  $\text{W}(\text{CO})_3(\text{PX}_3)_2(\text{CH}_2=\text{CH}_2)$  ( $\text{X} = \text{H}, \text{CH}_3, \text{F}, \text{Cl}, \text{Br}, \text{and I}$ ) (see **2**) were done at the BP86 level of pure density function theory [19]. The effective core potentials (ECPs) of Hay and Wadt with double- $\zeta$  valance basis sets (LanL2DZ) [20] were used to describe W, P, Cl, Br, and I. The 6-31g basis set was used for all other atoms [21]. Polarization functions were also added for Cl ( $\zeta_d = 0.514$ ), P ( $\zeta_d = 0.340$ ), Br ( $\zeta_d = 0.389$ ), I ( $\zeta_d = 0.266$ ), F ( $\zeta_d = 0.8$ ) [22], and C (ethylene and carbonyl) ( $\zeta_d = 1$ ). In all complexes, rotational barriers of ethylene were investigated by calculating the energy of various conformations corresponding to different values of the ethylene-carbonyl dihedral angle  $\theta$  (see **3**). For each value of  $\theta$  investigated, the rest of the geometry was relaxed. The harmonic vibrational frequencies of the different stationary points of the PES were calculated at the same level of theory in order to estimate the corresponding zero point vibrational energy (ZPE). All calculations were performed using the GAUSSIAN 98 software package [23]. The natural bond orbital (NBO)

analysis was used to evaluate the atomic charge and the bond hybridization [24]. NBO occupancies were used to quantitatively evaluate the occupation number of a given localized bonding/antibonding orbital, which gives information regarding to the strengths of interactions among different units within a molecule [24]. NBO calculations were performed with the NBO code [25] included in GAUSSIAN 98.

## 3. Results and discussion

To determine the rotational barrier of ethylene ligand, we optimized some various conformations of  $\text{W}(\text{CO})_3(\text{PX}_3)_2(\text{CH}_2=\text{CH}_2)$  ( $\text{X} = \text{H}, \text{CH}_3, \text{F}, \text{Cl}, \text{Br}, \text{and I}$ ) (**2**) complexes by DFT calculations (BP86) in the following orientations (see **3**):

1.  $\theta = 0^\circ$  (**1PX**)
2.  $\theta = 45^\circ$  (**2PX**)
3.  $\theta = 90^\circ$  (**3PX**)



### 3.1. $\text{W}(\text{CO})_3(\text{PX}_3)_2(\text{CH}_2=\text{CH}_2)$ ( $\text{X} = \text{H}, \text{CH}_3$ ) as models for $\text{W}(\text{CO})_3(\text{PCy}_3)_2(\text{CH}_2=\text{CH}_2)$ complex

As listed in Table 1, the selected optimized geometries of the model complex  $\text{W}(\text{CO})_3(\text{PH}_3)_2(\text{CH}_2=\text{CH}_2)$  (**3PH**) reproduced fairly well the geometries of the

Table 1

The optimized selected structural data (Å) for  $W(CO)_3(PH_3)_2(CH_2=CH_2)$  (**3PH** and **1PH**) and  $W(CO)_3(P(CH_3)_3)_2(CH_2=CH_2)$  (**3PCH3** and **1PCH3**) model complexes in comparison with corresponding experimental data of  $W(CO)_3(PCy_3)_2(\eta^2-C_2H_4)$  complex

	$r(W-C(a))_{av}$	$r(W-C(b))$	$r(W-P)_{av}$	$r(W-C)_{av}$ (ethylene)	$r(C-C)$ (ethylene)
<b>3PX</b>					
<b>3PH</b> (BP86)	2.032	2.007	2.464	2.381	1.416
<b>3PH</b> (B3PW91) <sup>a</sup>	2.008	1.985	2.491	2.365	–
<b>3PCH3</b> (BP86)	2.026	2.001	2.510	2.368	1.420
Exp <sup>b</sup>	2.010	1.977	2.555	2.338	1.378
<b>1PX</b>					
<b>1PH</b> (BP86)	2.037	1.991	2.457	2.444	1.398
<b>1PCH3</b> (BP86)	2.030	1.974	2.504	2.460	1.397

<sup>a</sup> Ref. [2].

<sup>b</sup> Ref. [8].

actual compound [12]. The calculated structural parameters at BP86 level are also relatively in well agreement with corresponding ones at B3PW91 level [6]. It is also interesting to know that  $W(CO)_3(P(CH_3)_3)_2-CH_2=CH_2$  (**3PCH3**) model complex is a better choice for mimicking the experimental phosphine geometry than **3PH** (Table 1). However, it is found that calculated bond distances in each model complex are systematically different with respect to the corresponding experimental complex (Table 1). Since this systematic error is very

likely to be reproduced in any of the compounds investigated here, it is expected that these results still elucidate relative trends in a reliable way.

The potential energy curves corresponding to the  $\eta^2$ -ethylene rotation of **PCH3** and **PH** calculated at BP86 level are shown in Figs. 1(a) and (b). The relative energies of all conformations of **PH** at BP86 level are also extensively in well agreement with the results obtained from B3PW91 level [6]. As discussed above, in these types of complexes, a perpendicular orientation between

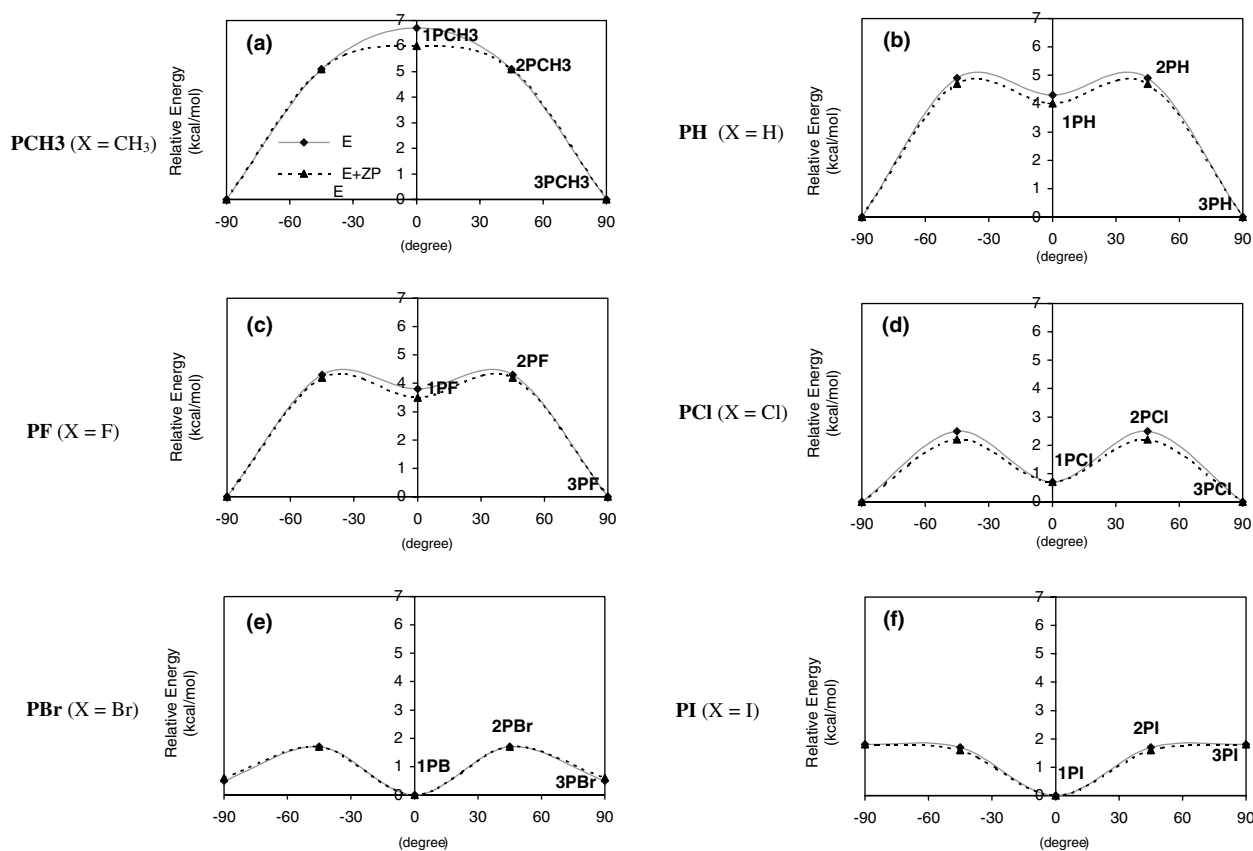


Fig. 1. Potential energy surfaces for complexes: (a) **PCH3**, (b) **PH**, (c) **PF**, (d) **PCI**, (e) **PBr**, and (f) **PI** showing the change in relative energies without zero-point energies ( $\Delta E$ ) and those with zero-point energies ( $\Delta E + ZPE$ ) with respect to  $\theta$  ( $^\circ$ ).

the alken's C–C vector and the OC–M–CO axis is preferred ( $\theta = 90^\circ$ ). It is found that, for **PH**, the potential energy curve reaches a maximum point when the C–C vector of  $\eta^2$ -ethylene ligand is in a staggered orientation with respect to the equatorial plane ( $\theta = 45^\circ$ ), while for **PCH3**, the maxima is coplanarity of the ethylene and the metal–carbonyl bonds ( $\theta = 0^\circ$ ).

Interestingly, one can clearly see that the W–C (ethylene) and W–C (carbonyl) bond distances are slightly shortened and simultaneously the C–C bond is slightly lengthened from **3PH** to **3PCH3** (Table 1). Since  $\text{PMe}_3$  is a stronger electron donor than  $\text{PH}_3$  [26], the W metal with  $\text{PMe}_3$  has more electrons available for  $\pi$ -backdonation to the  $\pi^*$  orbitals of the ethylene and carbonyl ligands, which strengthens the W–C interactions. Therefore, one expects that **3PCH3** would be more stable than **3PH**. To confirm this, we compared energy values  $E_{\text{TOT}}(\mathbf{3PCH3}) + 2E_{\text{TOT}}(\text{PH}_3)$  with  $E_{\text{TOT}}(\mathbf{3PH}) + 2E_{\text{TOT}}(\text{PMe}_3)$ , where  $E_{\text{TOT}}(\mathbf{3PCH3})$  and  $E_{\text{TOT}}(\mathbf{3PH})$  are the total electronic energies of **3PCH3** and **3PH**; and  $E_{\text{TOT}}(\text{PH}_3)$  and  $E_{\text{TOT}}(\text{PMe}_3)$  are the total electronic energies of the isolated ligands of  $\text{PH}_3$  and  $\text{PMe}_3$ . This calculation shows that **3PCH3** is more stable than **3PH** by 14.2 kcal/mol.

### 3.2. Comparison of important MOs of three conformations of $W(\text{CO})_3(\text{PH}_3)_2(\text{CH}_2=\text{CH}_2)$

All complexes considered here can be described as *pseudo*-octahedral structures. The MO calculations for three selected conformations of model complex **PH** (**1PH**, **2PH** and **3PH**) indicate that the three highest

occupied MOs correspond to the so-called “ $t_{2g}$ ” set orbitals (Fig. 2). Examination of other complexes almost gives the similar results. For **1PH**, the HOMO-2 represents the metal–ethylene  $d-\pi^*$   $\pi$ -bonding interaction. The HOMO and HOMO-1, which are the  $d_{xz}$  and  $d_{xy}$  orbitals, respectively, are nonbonding with respect to the  $\text{C}=\text{C}$   $\pi^*$  orbital of the ethylene ligand. In **3PH**, the metal–ethylene  $\pi$ -bonding interaction involves the  $d_{xz}$  orbital and lowers it to the HOMO-2. For this conformation (**3PH**), both  $d_{xy}$  and  $d_{yz}$  orbitals also remain nonbonding with respect to  $\pi^*$  orbital of the ethylene ligand. When  $\theta = 45^\circ$  (**2PH**), both the  $d_{xz}$  and  $d_{yz}$  orbitals are involved to some extent with  $\text{C}=\text{C}$   $\pi^*$  orbital, which causes these orbitals become somewhat stable in comparison with the  $d_{xz}$  orbital of **1PH** and the  $d_{yz}$  orbital of **3PH**. For all conformations, both the  $d_{yz}$  and  $d_{xy}$  orbitals of the metal center also interact with the two perpendicular  $\pi^*$  orbitals of carbonyl ligands, which are *cis* to ethylene ligand.

As shown in Fig. 2, in **1PH**, each unoccupied  $\pi$ -antibonding orbital of the CO and ethylene ligands interacts with  $d_{yz}$  orbital, while in **3PH**, the  $d_{xz}$  orbital interacts with ethylene  $\pi^*$  orbital and to some extent with  $\text{PH}_3$   $\sigma^*$  orbital. Since CO is a much stronger  $\pi$ -acceptor than  $\text{PH}_3$  ligand, thus, it is expected from **3PH** to provide a more suitable position for maximum backbonding interaction between the metal center and ethylene ligand. In other words, coplanarity of the ethylene with phosphine ligands, due to stronger metal–ethylene interaction, is more preferable than that of with carbonyl ligands. In **2PH**, because of an unsuitable orientation of ethylene ligand with respect to

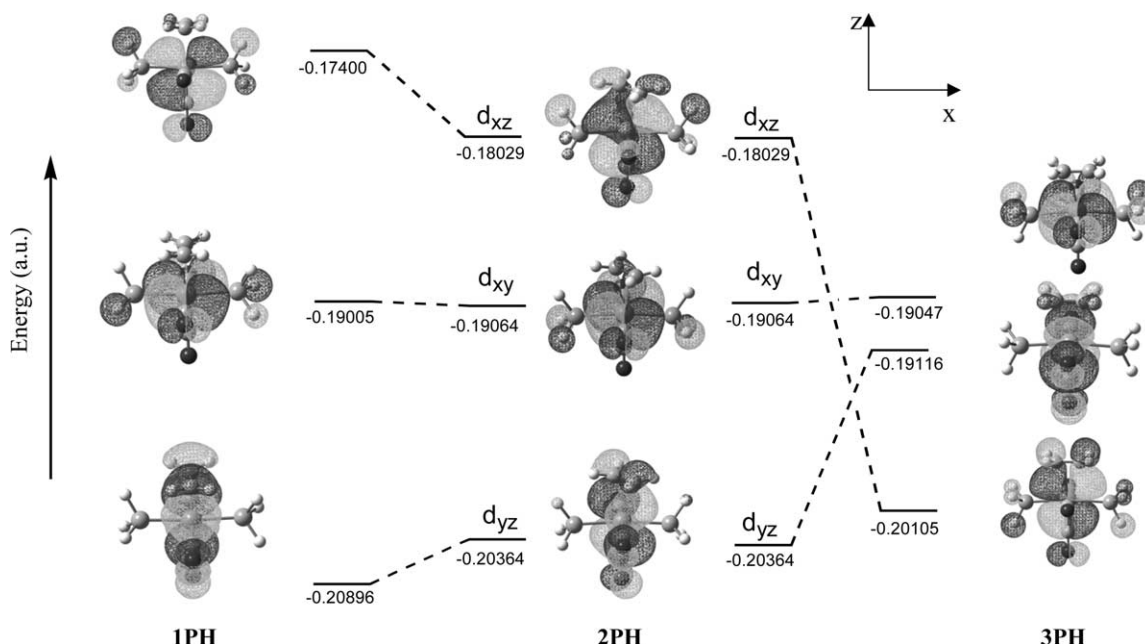


Fig. 2. Correlation diagram between the important MOs of conformations **1PH**, **2PH** and **3PH**.

W(CO)<sub>3</sub>(PH<sub>3</sub>)<sub>2</sub> fragment, there is a weaker interaction between ethylene π\* orbital and both the d<sub>xz</sub> and d<sub>yz</sub> orbitals compared to other conformations. In addition, in each three conformation of **PH**, the extent of the d<sub>xy</sub> orbital energy is almost the same; indicating that interaction between the ethylene π bonding electrons and electrons from d<sub>xy</sub> orbital has no effect on the destabilization of conformation **2PH**.

### 3.3. W(CO)<sub>3</sub>(PX<sub>3</sub>)<sub>2</sub>(CH<sub>2</sub>=CH<sub>2</sub>) (X = F, Cl, Br, and I)

W(CO)<sub>3</sub>(PX<sub>3</sub>)<sub>2</sub>(CH<sub>2</sub>=CH<sub>2</sub>) (X = F, Cl, Br, and I) complexes (see **2**) were used to investigate the rotational barrier of the ethylene. The corresponding potential energy surfaces are shown in Fig. 1. For **PF** and **PCI**, the minimum energy geometries occur when the ethylene ligand is coplanar with phosphine ligands. The potential energy surfaces for complexes **PBr** and **PI** show a conformation with minimum energy with the ethylene group eclipsed to carbonyl ligands. This is an interesting result, as it suggests that the type of phosphine ligand plays a role in determining the ethylene-phosphine arrangement. For conformations **3PX** and **1PX** of these complexes, the important bond lengths are summarized in Table 2.

Examining structural changes from **PH** and **PCH3** to the halide phosphine complexes, it is evident that W–P bond distances are shortened (see Tables 1 and 2), e.g., in conformations **3PH** and **3PCH3** the W–P bond distances are about 2.464 and 2.510 Å, which they drop to about 2.374, 2.413, 2.431, and 2.453 Å in **3PF**, **3PCI**, **3PBr**, and **3PI**. This behavior can probably be related to π-accepting ability of halide phosphines.

### 3.4. Bonding nature of complexes

Natural bond orbital analysis was adopted here to investigate the occupancy number of each NBO, which is expected to be useful for discussing the bonding nature. The occupancy numbers of several important NBOs are listed in Table 3, where the abbreviation of π-NBO, π\*-NBO, σ-NBO, and σ\*-NBO are adopted for π-bonding C=C NBO, its antibonding counterpart, σ-bonding W–C (ethylene) NBO, and its antibonding counterpart, respectively, hereafter. The occupancy numbers of the π-NBO and π\*-NBO are near 2.0 and 0.0, respectively, in free ethylene. In each conformation **1PX**, the occupancy number of π-NBO is significantly smaller but the occupancy number of π\*-NBO is significantly larger than that of the free ethylene. These

Table 2

The optimized selected structural data (Å) for conformations **3PX** and **1PX** of halide phosphine complexes W(CO)<sub>3</sub>(PX<sub>3</sub>)<sub>2</sub>(CH<sub>2</sub>=CH<sub>2</sub>) obtained from BP86 calculations

	r(W–C(a))	r(W–C(b))	r(W–P)	r(W–C) (ethylene)	r(C–C) (ethylene)
<b>3PX</b>					
<b>3PF</b>	2.043	2.015	2.374	2.412	1.409
<b>3PCI</b>	2.047	2.012	2.413	2.437	1.401
<b>3PBr</b>	2.048	2.009	2.431	2.445	1.398
<b>3PI</b>	2.048	2.004	2.453	2.454	1.395
<b>1PX</b>					
<b>1PF</b>	2.049	2.004	2.371	2.458	1.397
<b>1PCI</b>	2.053	2.005	2.401	2.461	1.395
<b>1PBr</b>	2.054	2.005	2.415	2.460	1.394
<b>1PI</b>	2.054	2.003	2.436	2.459	1.393

Table 3

Occupancies of NBOs of all conformations **1PX** and **3PX**

PX	Species	π(C–C)	π*(C–C)	σ(W–C)	σ*(W–C)
<b>1PX</b>	<b>1PCH3</b>	1.774	0.285	0.0	0.0
	<b>1PH</b>	1.758	0.286	0.0	0.0
	<b>1PF</b>	1.736	0.249	0.0	0.0
	<b>1PCI</b>	1.732	0.234	0.0	0.0
	<b>1PBr</b>	1.733	0.233	0.0	0.0
	<b>1PI</b>	1.738	0.231	0.0	0.0
<b>3PX</b>	<b>3PCH3</b>	0.0	0.0	1.776	0.661
	<b>3PH</b>	0.0	0.0	1.770	0.669
	<b>3PF</b>	0.0	0.0	1.746	0.670
	<b>3PCI</b>	0.0	0.0	1.694	0.702
	<b>3PBr</b>	1.724	0.261	0.0	0.0
	<b>3PI</b>	1.735	0.249	0.0	0.0

results are consistent with our understanding that the ethylene coordinates with the metal center through  $\sigma$ -donation and  $\pi$ -backdonation interactions. The occupancy numbers of the  $\pi$ -NBO and  $\pi^*$ -NBO in **1PCH3** and **1PH** are much larger than those of corresponding halide phosphine complexes (**1PF**, **1PCI**, **1PBr**, and **1PI**). This tendency clearly indicates that in **1PCH3** and **1PH**,  $\pi$ -backdonations become stronger than those of the halide phosphine analogs, while in both conformations, electron donations become weaker. This can be rationalized on the basis of the stronger  $\pi$ -accepting properties of the halide phosphine ligands, which effectively “pull” electron density from the metal center, which in turn allow for lower backdonations of metal electron density to ethylene and, on the other hand, more  $\sigma$ -donations of ethylene ligand to metal center. In addition, it is interesting to know that the occupancy number of the metal–C (ethylene) NBO ( $\sigma$ -NBO) is evaluated to be zero. This result suggests that though the C=C bond in conformations **1PX** becomes weaker than that in free ethylene, the  $\pi$ -bonding character is still maintained.

In **3PCI**, **3PF**, **3PH**, and **3PCH3** the occupancy number of  $\pi$ -NBO completely disappears, while the occupancy number of the C–C  $\sigma$ -NBO is near 2. In addition, the occupancy number of  $\sigma$ -NBO is 1.694, 1.746, 1.770, and 1.776 for **3PCI**, **3PF**, **3PH**, and **3PCH3**, respectively, and 0.702, 0.670, 0.669, and 0.661 for their antibonding counterparts ( $\sigma^*$ -NBO). From these occupancy numbers, it should be concluded that these conformations are characterized to be a tree-member metallacycle complex that involves the C–C single bond and the W–C (ethylene) covalent bond. These results are consistent with the notation that, for the complexes **PCI**, **PF**, **PH**, and **PCH3**, the eclipsed conformations have stronger metal–ethylene interaction and, consequently, are more stable. The NBO calculations, on the other hand, for **3PBr** and **3PI** indicate that the C=C double bond is maintained and the bond is formed through  $\sigma$ -donation and  $\pi$ -backdonation like their corresponding conformations **1PX**. It is interesting to note that, however, the occupancy number of  $\pi^*$ -NBO in **3PBr** and **3PI** are larger than that of **1PBr** and

**1PI**. The changes of C–C (ethylene) and W–C (ethylene) bond distances, listed in Tables 1 and 2, also confirm the above-discussed results. Examining the structural changes from **1PX** to **3PX**, one can easily find that the W–C (ethylene) bond distance is shortened, while the C–C (ethylene) bond distance is lengthened. These changes can be related to the increase of the amount of backdonation from the metal center into the  $\pi^*$ -orbital of ethylene when going from **1PX** to **3PX**. These results oppose the fact that in **PBr** and **PI**, the coplanar orientation of the ethylene and carbonyl ligand is preferred. On the basis of these results, it seems that in addition to electronic effects, the steric repulsive interactions resulted from bulky halide phosphines, **PX<sub>3</sub>** (X = Br and I), can also affect instabilities of conformations **3PX**.

### 3.5. Which factors are the origin of these structural preferences in the complexes?

To understand this structural behavior, we consider the energy of  $d_{xy}$  orbital in **3PX** as well as the energy difference between the  $d_{xz}$  orbital in **1PX** and the  $d_{yz}$  orbital in **3PX** ( $\Delta 1$ ). Since the  $d_{xy}$  orbital only participates in the  $\pi$ -backdonation with phosphine and *cis*-carbonyl ligands with respect to ethylene, its energy value can be a useful criterion on the extent of  $\pi$ -backdonation interaction. For complexes **3PX**, the energy of  $d_{xy}$  orbitals decrease in the order of **3PF** > **3PCI** > **3PBr** > **3PI**  $\gg$  **3PH** > **3PCH3**, which clearly shows that more  $\pi$ -acceptor **PX<sub>3</sub>** ligands are able to stabilize the  $d_{xy}$  orbital in complexes **3PX** because of better  $\pi$ -backdonation overlap. The  $\Delta 1$  energy differences also show the same trend (see Table 4). Therefore, it is expected that the W–P  $\pi$ -backdonation interaction becomes stronger in the order of **P(Me)<sub>3</sub>** < **PH<sub>3</sub>**  $\ll$  **PI<sub>3</sub>** < **PBr<sub>3</sub>** < **PCl<sub>3</sub>** < **PF<sub>3</sub>**.

For further argument and evaluation of the above results, the natural population analysis was calculated for all complexes. In conformations **3PX**, electron population of phosphine decreases upon the coordination with the W center and its positive charge becomes larger in the following order: **PI<sub>3</sub>** (0.221) < **PBr<sub>3</sub>** (0.238) < **PCl<sub>3</sub>**

Table 4

Orbital energies (a.u.) of  $d_{xy}$  and  $d_{yz}$  in **3PX** and those of  $d_{xz}$  in **1PX** as well as the energy difference between the  $d_{xz}$  orbital in **1PX** and the  $d_{yz}$  orbital in **3PX** ( $\Delta 1$ )

	$E(d_{xz})$ in <b>1PX</b>	$E(d_{yz})$ in <b>3PX</b>	$E(d_{xy})$ in <b>3PX</b>	$e1 - e2$
	<i>e1</i>	<i>e2</i>	<i>e3</i>	$\Delta 1$
<b>PCH3</b>	-0.14613	-0.17403	-0.16678	0.02790
<b>PH</b>	-0.17400	-0.19116	-0.19047	0.01716
<b>PF</b>	-0.22303	-0.22344	-0.24701	0.00041
<b>PCI</b>	-0.22451	-0.22534	-0.23689	0.00083
<b>PBr</b>	-0.22243	-0.22414	-0.23317	0.00171
<b>PI</b>	-0.21938	-0.22262	-0.22808	0.00324

(0.261)  $\ll$  PH<sub>3</sub> (0.393) < PF<sub>3</sub> (0.407) < P(Me)<sub>3</sub> (0.452). Other conformations, **2PX** and **1PX**, would also follow similar trend. However, this tendency is not consistent with above-mentioned  $\pi$ -accepting abilities of phosphine ligands. These population changes are understood on the basis of the fact that not only the  $\pi$ -backdonation but also the  $\sigma$ -donation contributes toward the coordination of phosphine to the W metal. From the results of calculations, it should be concluded that the  $\sigma$ -donation of halide phosphine ligands increase in the order of PI<sub>3</sub> < PBr<sub>3</sub> < PCl<sub>3</sub>  $\ll$  PF<sub>3</sub>, while  $\pi$ -accepting ability of halide phosphines decrease along the series PF<sub>3</sub> > PCl<sub>3</sub> > PBr<sub>3</sub> > PI<sub>3</sub>. The increasing order of above-mentioned  $\sigma$ -donation is understood in terms of the percent of polarized electron toward the W center in the W–P  $\sigma$ -bond, which decreases in the following manner: PF<sub>3</sub> (%37.61)  $\gg$  P(Me)<sub>3</sub> (%32.56) > PCl<sub>3</sub> (%30.50) > PH<sub>3</sub> (%30.18) > PBr<sub>3</sub> (%30.08) > PI<sub>3</sub> (%29.33). This is in accord with the recent calculation by Frenking and co-workers [18] which showed donation of phosphine ligand in Fe(CO)<sub>4</sub>PF<sub>3</sub> to be higher than donation in Fe(CO)<sub>4</sub>PH<sub>3</sub>.

Comparing the potential energy surfaces of all complexes with each other, one can easily find that the energy differences between conformations **3PX** and **1PX** increase in the order of **PI** (–1.8 kcal/mol) < **PBr** (–0.5 kcal/mol) < **PCI** (0.7 kcal/mol) < **PF** (3.8 kcal/mol) < **PH**

(4.3 kcal/mol) < **PCH3** (6.7 kcal/mol). The results of calculations imply that the strong electron donor and the weak electron  $\pi$ -acceptor properties of a phosphine ligand enhance interaction between the metal center and ethylene ligand compared to those phosphine ligands having weaker electron donor and stronger electron  $\pi$ -acceptor, e.g., in **3PMe3**, W–C (ethylene) bond distance, 2.368 Å, is smaller than that of other phosphine complexes (2.381, 2.412, 2.437, 2.445, and 2.454 Å in **3PH**, **3PF**, **3PCI**, **3PBr**, and **3PI**, respectively), indicating that the extent of interaction between the W metal and the ethylene ligand decreases in the order of **3PCH3** > **3PH** > **3PF** > **3PCI** > **3PBr** > **3PI**. The same trend is also supported from the results of NBO analysis (see Table 3) and C–C (ethylene) bond distance (see Tables 1 and 2).

As mentioned above, in the complexes containing halide phosphines the energy difference between **3PX** and **1PX** as well as W–ethylene interaction in **3PX** decrease by increasing the size of the halogen atom (see Fig. 1 and Table 3). This seems unexpected, due to the fact that the  $\pi$ -accepting abilities of halide phosphines increase by substitutes X up the group of VII. Some tentative explanations are given below, though other explanations are also possible. In the complex **PF**, on one hand, the W–phosphine  $\pi$ -backdonation interaction is expected to be the strongest, on the basis of the MO

Table 5

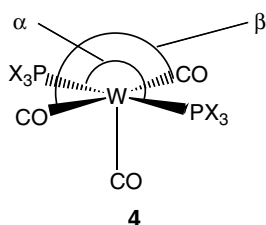
P–W–P and C–W–C bond angles (°) of complexes **PX** and naked complexes **PX** as well as P–W–P(**PX**)–P–W–P(naked **PX**) ( $\Delta\alpha$ ), C–W–C(**PX**)–C–W–C(naked **PX**) ( $\Delta\beta$ ),  $\Delta\alpha(3PX) - \Delta\alpha(1PX)$  ( $\Delta\Delta\alpha$ ), and  $\Delta\beta(3PX) - \Delta\beta(1PX)$  ( $\Delta\Delta\beta$ ) of corresponding complexes

	P–W–P ( $\alpha$ )	C–W–C ( $\beta$ )	P–W–P( <b>PX</b> )–P–W–P(naked <b>PX</b> ) ( $\Delta\alpha$ )	C–W–C( <b>PX</b> )–C–W–C(naked <b>PX</b> ) ( $\Delta\beta$ )	$\Delta\alpha(3PX) - \Delta\alpha(1PX)$ ( $\Delta\Delta\alpha$ )	$\Delta\beta(3PX) - \Delta\beta(1PX)$ ( $\Delta\Delta\beta$ )
<b>PF</b>						
<b>1PF</b>	178.6	185.7	–3.5	8.7		
<b>3PF</b>	185.2	177.1	3.1	0.1	6.6	–7.7
Naked <b>PF</b>	182.1	177.0	–	–		
<b>PCI</b>						
<b>1PCI</b>	179.5	186.0	3.1	6.0		
<b>3PCI</b>	186.4	177.6	9.7	–2.4	6.6	–8.4
Naked <b>PCI</b>	176.7	180.0	–	–		
<b>PBr</b>						
<b>1PBr</b>	180.4	186.4	5.8	4.7		
<b>3PBr</b>	186.2	178.4	11.6	–3.3	5.8	–8.0
Naked <b>PBr</b>	174.6	181.7	–	–		
<b>PI</b>						
<b>1PI</b>	181.6	187.0	9.8	3.0		
<b>3PI</b>	186.5	179.6	14.7	–4.4	4.9	–7.4
Naked <b>PI</b>	171.8	184.0	–	–		
<b>PH</b>						
<b>1PH</b>	177.3	186.5	–0.1	6.0		
<b>3PH</b>	186.6	176.9	9.2	–3.6	9.3	–9.6
Naked <b>PH</b>	177.4	180.5	–	–		
<b>PCH3</b>						
<b>1PCH3</b>	181.5	186.3	9.8	2.7		
<b>3PCH3</b>	190.9	177.0	19.2	–6.6	9.4	–9.3
Naked <b>PCH3</b>	171.7	183.6	–	–		

results and, on the other hand, the electron donation of  $\text{PF}_3$  ligand is highest at the same time. The former case decreases the amount of electrons available for  $\pi$ -backdonation to  $\pi^*$  orbital of ethylene while the latter case increases it. These results indicate that the  $\text{PF}_3$  ligand provides the optimal balance between the W metal and the ethylene interaction. Examining results obtained from NBO analysis, it can be concluded that other halide phosphine ligands have much weaker  $\sigma$ -donation ability than  $\text{PF}_3$  ligand ( $\text{PF}_3 \gg \text{PCl}_3 > \text{PBr}_3 > \text{PI}_3$ ), consequently, one expects that metal–ethylene  $\pi$ -backdonation interaction becomes weaker when moving down the column VII from  $X = \text{F}$  to I.

In addition, as listed in Table 5, P–W–P bending angle ( $\alpha$ ) of the naked halide complexes,  $\text{W}(\text{CO})_3(\text{PX}_3)_2$  (see **4**), which are optimized at BP86 level, decreases and simultaneously C–W–C bending angle ( $\beta$ ) increases when going from  $X = \text{F}$  to I. Based on the results of calculations, it can be observed that structural changes between the reactants,  $\text{W}(\text{CO})_3(\text{PX}_3)_2$ , and their corresponding conformations **3PX** ( $\Delta\alpha$  and  $\Delta\beta$ ) increase as one moves down the VII column from  $X = \text{F}$  to I, while the cited differences relative to those of analogs between reactant and **1PX**,  $\Delta\Delta\alpha$  and  $\Delta\Delta\beta$ , do not have significant changes (see Table 5). Therefore, one could expect, in halide phosphine complexes, particularly in **PBr** and **PI**, part of the energy difference between **3PX** and **1PX** as well as the extent of W–ethylene interaction in **3PX** to originate from the fact that conformations **3PX** are destabilized by the increased repulsion between larger halide phosphines and carbonyl ligands because, in a conformation **3PX** with the bulky halide phosphines, the coordinating ethylene leads to significant structural changes.

It is surprising that, despite the high observed structural change, **3PCH3** shows a strong W–ethylene interaction compared to **1PCH3**, much higher than that of **3PF** and **3PH**. It seems that the very weak  $\pi$ -acceptor and strong electron donor properties of  $\text{P}(\text{Me})_3$  ligands are able to compensate for high structural change in **3PCH3**.



#### 4. Conclusions

The preference for coplanarity of the ethylene and one of the metal–ligand bonds in complexes  $\text{W}(\text{CO})_3(\text{PX}_3)_2(\text{CH}_2=\text{CH}_2)$  ( $X = \text{H}, \text{CH}_3, \text{F}, \text{Cl}, \text{Br},$  and

I) have been investigated by density functional theory calculations. The effects of substituent X of phosphine ligands have been examined. The structural parameters calculated for  $\text{W}(\text{CO})_3(\text{P}(\text{CH}_3)_3)_2(\text{CH}_2=\text{CH}_2)$  are in good agreement with the experimental observation in comparison with other complexes. For ethylene complexes containing  $\text{PCl}_3, \text{PF}_3, \text{PH}_3,$  and  $\text{P}(\text{Me})_3$ , the C–C vector of ethylene ligand prefer to be coplanar with P–W–P axis, while structural preference of those containing  $\text{PBr}_3$  and  $\text{PI}_3$  ligands are coplanarity of the ethylene and carbonyl ligands.

The results obtained from MO calculation and NBO analysis indicate that the  $\pi$ -accepting properties of phosphines increase in the order of  $\text{P}(\text{Me})_3 < \text{PH}_3 \ll \text{PI}_3 < \text{PBr}_3 < \text{PCl}_3 < \text{PF}_3$ , while their electron donation decrease in the order of  $\text{PF}_3 \gg \text{P}(\text{Me})_3 > \text{PCl}_3 > \text{PH}_3 > \text{PBr}_3 > \text{PI}_3$ . These calculations also imply that the amount of  $\pi$ -backdonation from W metal to  $\pi^*$ -orbital of ethylene ligand increases in the order of **3PCH3** > **3PH** > **3PF** > **3PCI** > **3PBr** > **3PI**. The W–ethylene  $\pi$ -backdonation interaction also increases from **1PX** to **3PX**.

Apparently, in halide phosphine complexes, particularly in complexes including  $\text{PBr}_3$  and  $\text{PI}_3$ , in addition to the electronic effects, the steric factors also control the orientation of ethylene in complexes. Examining results of calculations, it is also suggested that the very weak  $\pi$ -acceptor and strong electron donor properties of  $\text{P}(\text{Me})_3$  ligands enhance W–ethylene  $\pi$ -backdonation interaction and consequently, compensate for steric factors resulted from bulky groups of  $\text{P}(\text{Me})_3$  ligands.

#### Acknowledgements

The support of SGS cooperation is gratefully acknowledged. A. Ariaferd thanks Professor Zhenyang Lin and Xin Huang, Hong Kong university of Science and Technology and Mr. Said Madeh Khaksar, Nashre Mowzoon-Iran, for their fruitful discussion.

#### References

- [1] (a) L.K. Johnson, C.M. Killian, M. Brookhart, J. Am. Chem. Soc. 117 (1995) 6414;  
(b) A.S. Abu-Surrah, B. Riegler, Angew. Chem., Int. Ed. Engl. 35 (1996) 2475.
- [2] B.R. James, Homogenous hydrogenation, Wiley, New York, 1973, p. 314.
- [3] J. Smidt, W. Hafner, R. Jira, R. Sieber, J. Sedlmeier, A. Sable, Angew. Chem. 74 (1962) 93.
- [4] T. Ziegler, V. Tschinke, in: Bonding Energetic in Organometallic Compounds, in: T.J. Marks (Ed.), ACS Symposium Series, Vol. 428, American Chemical Society, Washington, DC, 1990 (Chapter 19).



- [5] (a) M.J.S. Dewar, *Bull. Soc. Chem. Fr.* (1951) C71;  
(b) J. Chatt, L.A. Duncanson, *J. Chem. Soc.* (1953) 2939.
- [6] W.H. Lam, Z. Lin, *J. Organomet. Chem.* 635 (2001) 84.
- [7] S.-H. Choi, I. Bytheway, G. Jia, Z. Lin, *Organometal.* 17 (1998) 3974.
- [8] M.-F. Fan, Z. Lin, G. Jia, *J. Am. Chem. Soc.* 118 (1996) 9915.
- [9] S.-H. Choi, Z. Lin, *Organometallics* 18 (1999) 2473.
- [10] M. Oliván, E. Clot, O. Eisenstein, K.G. Caulton, *Organometallics* 17 (1998) 897.
- [11] S. Li, M.B. Hall, J. Eckert, C.M. Jensen, A. Albinati, *J. Am. Chem. Soc.* 122 (2000) 2903.
- [12] M.D. Butts, J.C. Bryan, X.-L. Luo, G.J. Kubas, *Inorg. Chem.* 36 (1997) 3341.
- [13] H. Berke, G. Huttner, C. Sontag, L. Zsolnai, *Z. Naturforsch.* 40b (1985) 799.
- [14] H.-F. Hsu, Y. Du, T.E. Albrecht-Schmitt, S.R. Wilson, J.R. Shapley, *Organometallics* 17 (1998) 1756.
- [15] R.H. Crabtree, *The Organometallic Chemistry of the Transition Metals*, second ed., Wiley, New York, 1994, p. 71.
- [16] T. Kinnunen, K. Laasonen, *J. Organomet. Chem.* 665 (2003) 150.
- [17] G. Frison, H. Grutzmacher, *J. Organomet. Chem.* 643–644 (2002) 285.
- [18] Y. Chen, M. Hartmann, G. Frenking, *Z. Anorg. Allg. Chem.* 627 (2001) 985.
- [19] (a) A.D. Becke, *Phys. Rev. A* 38 (1988) 3098;  
(b) J.P. Perdew, *Phys. Rev. B* 33 (1986) 8822;  
(c) J.P. Perdew, *Phys. Rev. B* 34 (1986) 7406.
- [20] P.J. Hay, W.R. Wadt, *J. Chem. Phys.* 82 (1985) 299.
- [21] P.C. Hariharan, J.A. Pople, *Theor. Chim. Acta* 28 (1973) 213.
- [22] S. Huzinaga, *Gaussian Basis Sets for Molecular Calculation*, Elsevier, Amsterdam, 1984.
- [23] M.J. Frisch, G.W. Trucks, H.B. Schlegel, G.E. Scuseria, M.A. Robb, J.R. Cheeseman, V.G. Zakrzewski, Jr., J.A. Montgomery, R.E. Stratmann, J.C. Burant, S. Dapprich, J.M. Millam, A.D. Daniels, K.N. Kudin, M.C. Strain, O. Farkas, J. Tomasi, V. Barone, M.C.R. Cossi, B. Mennucci, C. Pomelli, C. Adamo, S. Clifford, J. Ochterski, G.A. Petersson, P.Y. Ayala, Q. Cui, K. Morokuma, D.K. Malick, A.D. Rabuck, K. Raghavachari, J.B. Foresman, J. Cioslowski, J.V. Ortiz, A.G. Baboul, B.B. Stefanov, G. Liu, A. Liashenko, P. Piskorz, I. Komaromi, R. Gomperts, R.L. Martin, D.J. Fox, T. Keith, M.A. Al-Laham, C.Y. Peng, A. Nanayakkara, C. Gonzalez, M. Challacombe, P.M.W. Gill, B. Johnson, W. Chen, M.W. Wong, J.L. Andres, C. Gonzalez, M. Head-Gordon, E.S. Replogle, J.A. Pople, *GAUSSIAN 98*, Revision A.7, Gaussian, Inc., Pittsburgh, PA, 1998.
- [24] A. Reed, L.A. Curtiss, F. Weinhold, *Chem. Rev.* 88 (1988) 899.
- [25] E.D. Glendening, A.E. Read, J.E. Carpenter, F. Weinhold, *NBO* (version 3.1), Gaussian Inc., Pittsburgh, PA, 1998.
- [26] (a) J. Song, M.B. Hall, *J. Am. Chem. Soc.* 115 (1993) 327;  
(b) H. Jacobsen, H. Berke, *Chem. Eur. J.* 3 (1997) 881.